

Orientation and temperature dependences on fatigue crack growth (FCG)

behavior of a Ni-base directionally solidified superalloy

Yangyang Zhang¹, Huiji Shi^{1,*}, Jialin Gu², Changpeng Li³, Kai Kadau⁴, Oliver Luesebrink⁵

¹Department of Engineering Mechanics, Tsinghua University, Beijing 100084, China)

²Department of Material Science, Tsinghua University, Beijing 100084, China)

³Corporate Technology, Siemens Ltd. China, Beijing 100102, China)

⁴Siemens Energy Inc., Charlotte, USA)

⁵Siemens AG Energy, Mulheim an der Ruhr, Germany)

* Corresponding author. Email: shihj@mail.tsinghua.edu.cn

Abstract Fatigue crack growth (FCG) behaviors of a widely-used nickel-based directionally solidified (DS) superalloy were investigated. Direct-current potential drop method was employed to capture the crack length according to ASTM E647. Standard compact tension (CT) specimens in longitudinal, transverse and diagonal directions were cast and tested at T_0 and $T_0+250^{\circ}\text{C}$ to reveal the orientation and temperature dependence. Moreover, the post-test fractography were observed through SEM and OM to understanding the underlying mechanism responsible for the fracture modes. Results suggested that cracks in all three orientations propagated transgranularly, no obvious differences were found between each other, and thus, the orientation dependence appeared to be very weak, all da/dN - DK curves in three orientations fell into one narrow band. However, temperatures showed significant dependence in diagonal directions, while in transverse direction the dependence became weak and even none in longitudinal orientation. Finally, methods for characterizing the FCG behaviors in different orientations and at both temperatures were proposed, which were able to explain the orientation and temperature dependences.

Key words Fatigue crack growth, directionally solidification, nickel-based superalloy

1. Introduction

Superalloys, either in the conventionally-cast (CC) or directionally solidified (DS) forms may contain porosity and shrinkage cracks, so that the life of rotating components, such as turbine blades, may be limited by crack propagation from these defects. It is therefore of interest to determine the resistance of the oriented grain structure, produced by DS, to the propagation of fatigue cracks [1]. Although lots of research have been focused on the fatigue crack growth behaviors of superalloys, few have shed light on those behaviors of directionally solidified superalloys[1-6]. In 1976, Scarlin [1] investigated the fatigue crack growth behaviors of nickel-based IN738 DS, and high cycle fatigue crack growth rates had been measured at room and high temperatures and for crack propagation both parallel and perpendicular to the solidification directions. However, comparable crack growth rate seemed to be found in his results. Okazaki et al [2] conducted low cycle fatigue tests to study the stage-I short crack growth behavior RENE80+Hf and CM247LC DS at 600°C . Later, Highsmith et al [4, 6] and Yoon et al [5] studied the FCG behaviors of nickel-base GTD-111 DS, both in longitudinal and transverse directions, where the stress ratio effects and temperature effects were focused on, respectively. For DS material, it is seen that only crack growth in

longitudinal and transverse directions are interested and investigated. However, the diagonal direction is very often used as loading components during actual service; therefore more studies concerning this particular direction should be done.

The current DS material is a newly cast and wrought nickel-base directionally solidified (DS) superalloy, to meet the requirement for development of more efficient engine operation with higher operating temperatures and stresses. In the current paper, FCG behaviors of DS material have been evaluated at T_0 and $T_0+250^{\circ}\text{C}$, and in longitudinal, transverse and diagonal orientations. The effects of temperatures and grain orientations on the FCG behaviors are investigated in associated with fractographic analysis (For confidential, some of the test data are normalized).

2. Material and experimental procedure

The nominal chemical compositions of the material are listed in Table 1. The original slabs were directionally solidified to produce a longitudinal direction which corresponds to [001] crystal orientation. The directionally solidified direction along the axis of the bar was determined to be within 5° of dispersion using the X-ray diffraction technique.

Table 1. Nominal compositions of the current DS material (wt.%)

Al	B	C	Cr	Mo	Ta	Ti	W	Ni
3.40	0.0125	0.08	11.6	1.65	4.80	3.90	3.50	Bal.

FCG tests were conducted by using the direct-current electric potential drop method (DC-PDM) described in ASTM E647. Standard compact-tension (CT) specimens (48*50*10) were machined using electron-discharge machining techniques from the heat treated slabs. Prior to standard FCG tests, all specimens were pre-cracked at room temperature with a frequency of 10 Hz to eliminate the effect of machining notches. Lengths of all pre cracks were in a range of 2-3 mm. FCG tests were conducted in accordance with the requirements of ASTM E647 [7]. All tests were running loading control by a computer-control, closed-loop servo-hydraulic testing machine, with a fixed load ratio of 0.1 and frequency of 10 Hz. At both temperatures, two repeated specimens were tested in each grain orientation, one with standard FCG tests with constant loading, the other with threshold testing by decreasing loading, whose derating ratio is 0.1.

The crack length data in region II of each specimen, with or without threshold value test, are computed by two methods, i.e., the secant method (also known as point-to-point technique) as well as the seven-point incremental polynomial method, as described in [7]. Conventionally, the secant method gives a result that most reflects the actual conditions, such as crack growth rate change, fluctuation and so on, while the polynomial method produces a more smooth da/dN curve. In the subsequent analysis, results from the seven-point polynomial method will be used to compare the temperature as well as orientation effects.

For the standard C(T) specimens, the stress intensity factor ranges were calculated by the following equation as:

$$\Delta K = \frac{\Delta P}{B\sqrt{W}} \frac{(2+\alpha)}{(1-\alpha)^{3/2}} (0.886 + 4.64\alpha - 13.32\alpha^2 + 14.72\alpha^3 - 5.6\alpha^4) \quad (1)$$

where $\alpha = a/W$, a is computed crack length, W takes a constant value of 40, and P is the applied load.

3. Results and discussion

Three types of specimens with different orientations were machined from cast plates. Figure 1 indicates the schematic images of these three types of CT specimens, where the different-color cylinders indicate crystal grains. Totally 12 specimens were tested at T_0 and $T_0+250^\circ\text{C}$, with crack growth in longitudinal, transverse and diagonal directions, respectively.

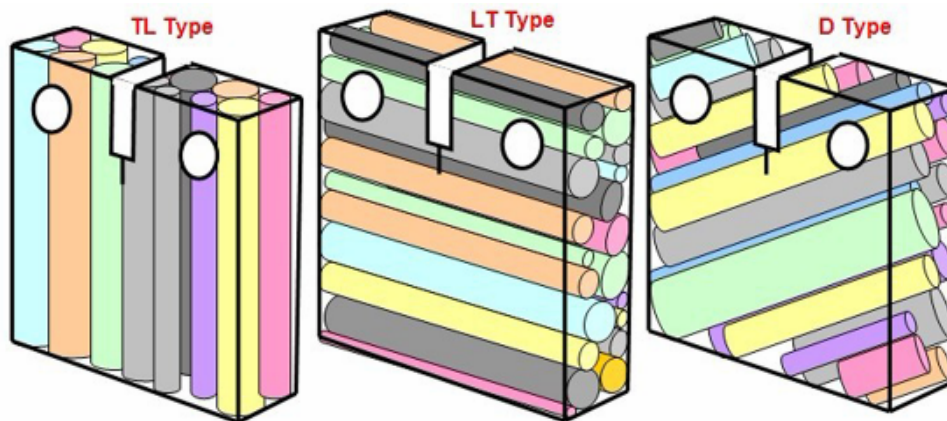


Figure 1. Schematic images of three types of C(T) specimens

3.1. Effect of orientation on FCG rates

The overall crack growth rate versus stress intensity factor values in Paris regime, i.e., $da/dN - \Delta K$ curves, are depicted in Figure 2, from which one can conclude that the orientation dependence is very weak, i.e., crack growth data in all orientations fall into one narrow [1/3, 3] band. Meanwhile, when using Paris law to obtain linear regression of all crack growth data, the correlation coefficient can be up to 0.88.

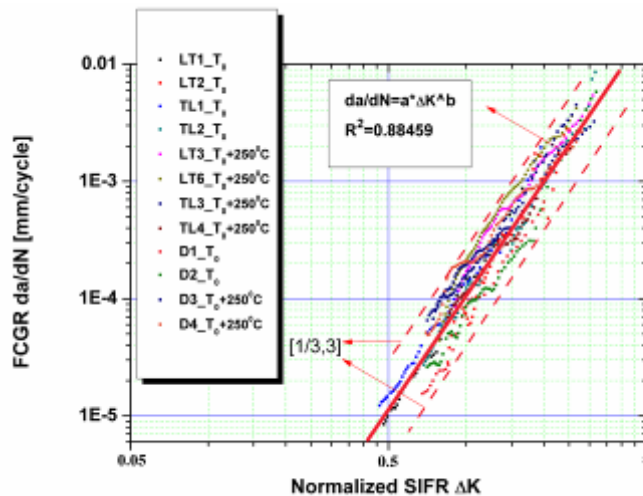


Figure 2. Fatigue crack growth behaviors for all DS specimens in Region II

Figure 3 shows the crack growth behaviors for the three types of specimens tested at T_0 . Generally, comparable crack growth rate data can be found in longitudinal and transverse directions, while those in diagonal direction seem to be lower, especially in the high- ΔK regime. That's to say, there is no significant difference between crack growth rate in longitudinal and transverse directions, while specimens in diagonal direction have a much lower crack growth rate, and the difference becomes larger when it is up to the high- ΔK regime.

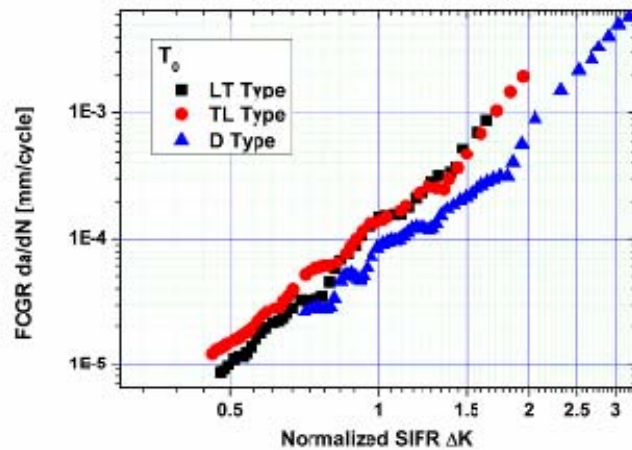


Figure 3. Crack growth behaviors of three types of specimens tested at T_0

However, at $T_0+250^\circ\text{C}$, the orientation dependence becomes even weaker, as can be seen in Figure 4. Cracks that travel in longitudinal and transverse directions also have a comparable crack growth rate; but different with those at T_0 , cracks in diagonal directions still travel with a comparable rate, and no obvious difference can be found, even in the high- ΔK regime.

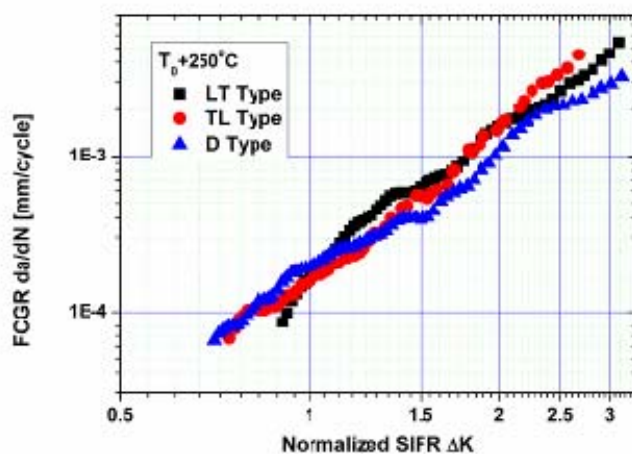


Figure 4. Crack growth behaviors of three types of specimens tested at $T_0+250^\circ\text{C}$

3.2. Effect of temperature on FCG rates

Figure 5 compares the growth rate of cracks traveling in longitudinal direction at both temperatures. In longitudinal direction, cracks seem to grow equally fast at both temperatures, and no obvious differences can be found between T_0 and $T_0+250^\circ\text{C}$.

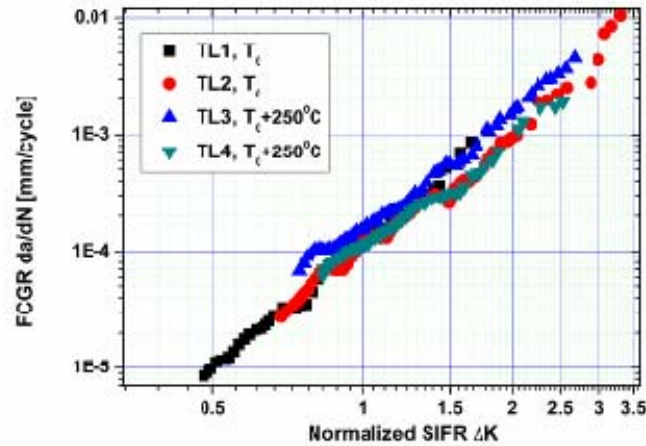


Figure 5. Crack growth behaviors of TL type specimens at T_0 and $T_0+250^\circ\text{C}$

In Figure 6, weak temperature dependence can be found on the LT type crack growth rate, i.e., cracks grow slightly faster at $T_0+250^\circ\text{C}$ than at T_0 .

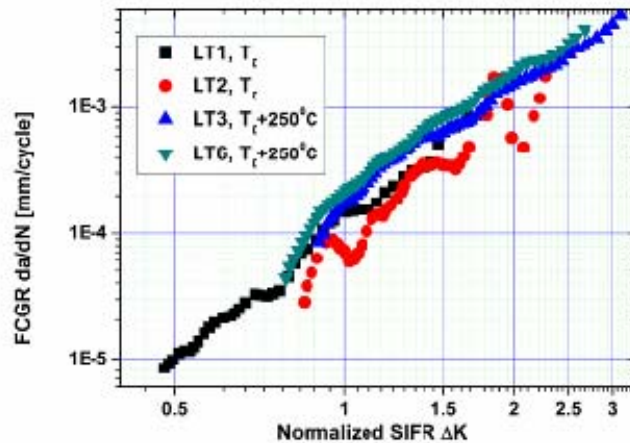


Figure 6. Crack growth behaviors of LT type specimens at T_0 and $T_0+250^\circ\text{C}$

Figure 7 compares the growth behaviors for diagonal cracks traveling both at T_0 and $T_0+250^\circ\text{C}$, from which one can conclude that apparent temperature effect can be found on the diagonal crack growth. Generally, cracks propagate much faster at $T_0+250^\circ\text{C}$ than at T_0 , especially in the low- ΔK regime. Subsequently, the growth rate at both temperatures become more and more close to each other as ΔK arise, and they take nearly the same value when normalized $\Delta K \approx 2.5$. After that, cracks at T_0 start to exceed those at $T_0+250^\circ\text{C}$, until the final break.

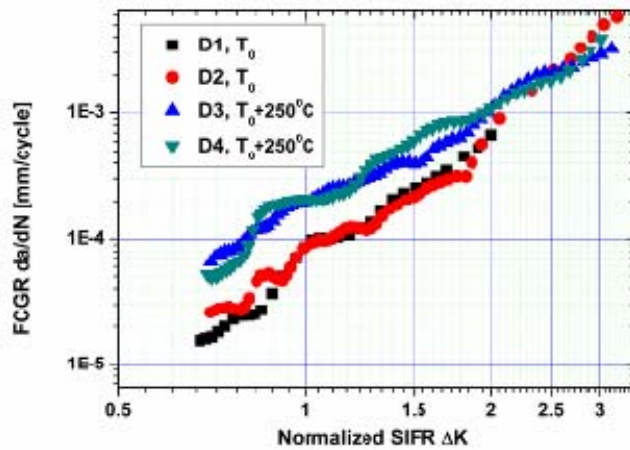


Figure 7. Crack growth behaviors of D type specimens at T_0 and $T_0+250^\circ\text{C}$

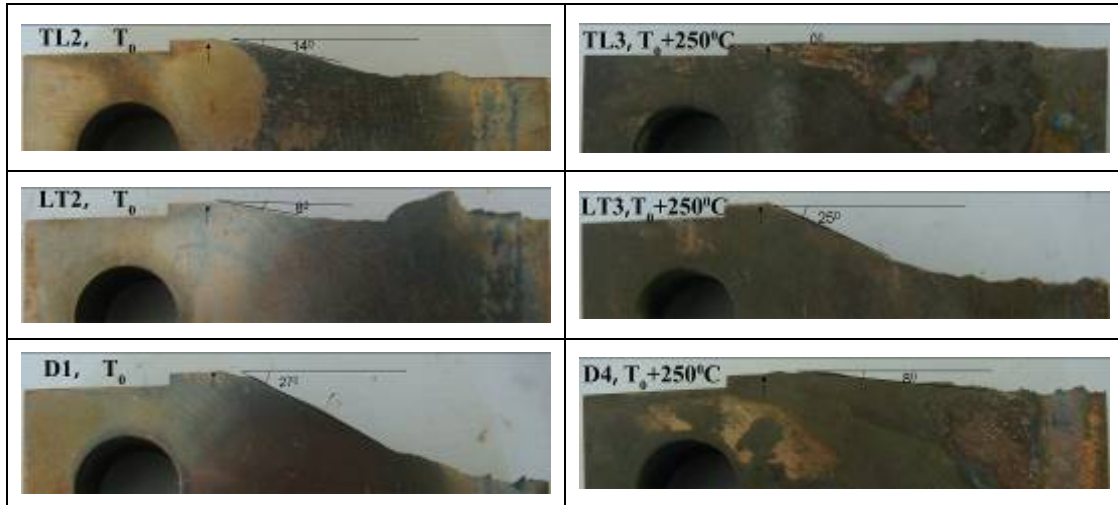
3.3. Fractography

All FCG tests were run until the specimen was separated into two parts. The fracture surfaces of all post-test specimens were observed through SEM and OM to understand the underlying mechanisms responsible for different damage modes. In regard to crack propagation behavior of single crystal superalloys, it is well known that cracks tend to propagate on $\langle 111 \rangle$ slip planes at low temperature, while cracks usually propagate normal to loading direction independent of crystal orientation at high temperature [8-11]. The former cracking behavior is called stage-I cracking, and the latter is called stage-II cracking. In current project, both stage-I and stage-II cracking modes can also be found, as can be seen by the side faces of fracture surfaces.

Table 2 lists the side faces of specimens tested at both temperatures, in which cracks propagated from left to right, and a black arrow in each figure corresponds to a machined notch tip. For TL type specimens (i.e., cracks propagate along the longitudinal direction), crack follow an angle of $\alpha \approx 14^\circ$ to the loading direction at T_0 , which seems as a stage-I cracking mode, while both at $T_0+250^\circ\text{C}$ show stage-II type of cracking modes. For LT type specimens (i.e., cracks travel along the transverse direction), trends are totally reversed, i.e., cracks at T_0 follow an angle of $\alpha \approx 8^\circ$ to the loading direction, while those at $T_0+250^\circ\text{C}$ all travel along a constant angle of $\alpha \approx 25^\circ$; For diagonal specimens, stage-I cracking mode can also be seen at lower temperature ($\alpha \approx 27^\circ$), while at higher temperature, cracking surfaces show stage-II type cracking mode ($\alpha \approx 8^\circ$). To sum up, cracks in different orientations show different cracking modes, namely, cracks travel along longitudinal and diagonal directions show stage-I cracking at lower temperature and stage-II cracking at higher temperature, which is in accordance with literature. However, cracks travel in

transverse direction show a different trend.

Table 2. Side faces of post-test specimens at T_0 and $T_0+250^\circ\text{C}$



Note that for all the fracture surfaces, no angles were found through the thickness direction, i.e., all fracture surfaces are totally perpendicular to the specimen surfaces, and no inclinations were found.

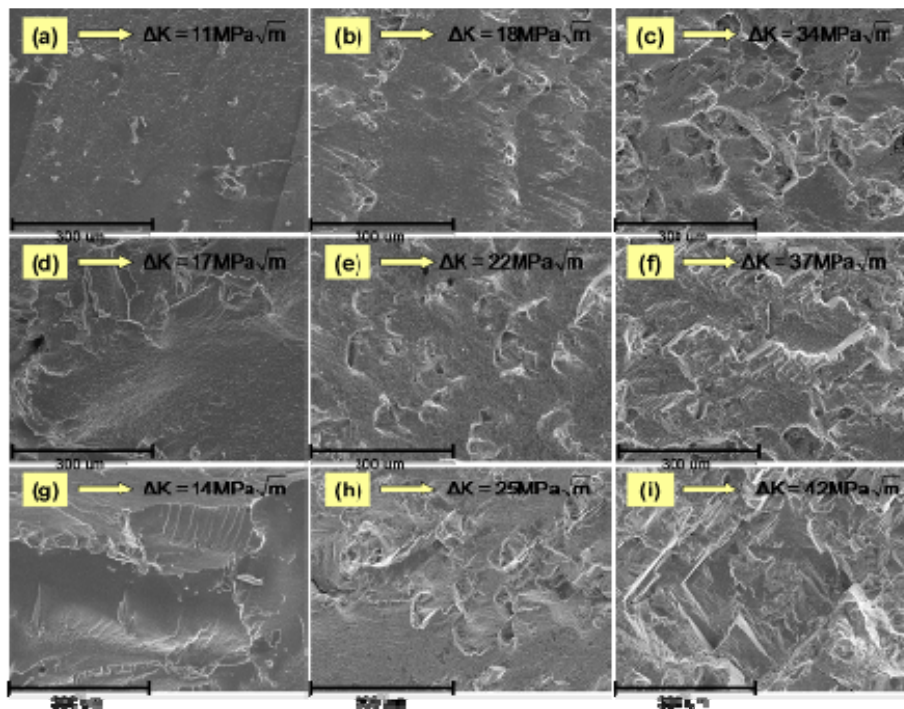


Figure 8. Fracture surfaces in various ΔK regimes at T_0 (a)-(c) TL type (d)-(f) LT type (g)-(i) D type

A more detailed examination results on the fracture surfaces in various ΔK regimes are presented in Figure 8. At low ΔK regimes, all fracture surfaces are smooth and very fine fatigue striations were observed on the fracture surfaces, indicating a slow but steady cracking stage, as can be seen in Figure 8 (a), (d) and (g); however, at higher ΔK regime a more textured fracture morphology with cracks was observed, and there were lots of claw-like barriers lying on the path (see Figure 8 (b), (e) and (h)).

and (h)). This type of barrier is very common for most the specimens in all three orientations, and it is supposed that the effect of this kind of barrier on crack growth is much more important than the crystal boundaries. As ΔK arises, extensive crystal facet formations have been found for all three orientations. The reasons may be, as ΔK become so large that the local barriers can hardly produce any effective resistance, thus a predominant crack can easily and quickly travel through a crystal grain, and the appearance of crystal facet is attributed to the need for rapid energy dissipation by the advancing crack. Such energy dissipation is the fastest when cracks travel along the easiest path, i.e., the slip facets of each grain.

Figure 9 shows the typical claw-like barriers that have been widely found in the crack paths. It is suggested that when crack tip starts to reach these local barriers, it has been stopped due to the existence of these barriers, and as cyclic loading going on, new cracks start to re-initiate from these barriers; Subsequently, as the new cracks keeps growing and finally coalesce with the original crack, these barriers are seen to be passed through. Therefore it is inferred that these claw-like barriers do play an important role in cracks growth, and sometimes the effect of these barriers are so huge that the role of grain boundaries can hardly be seen. Besides, worth mentioning that in the previous pre-test procedure where some same C(T) specimens made of CM 247LC DS were conducted FCG tests, very few or no claw-like barriers had been found in their crack paths, so those specimens showed significant orientation dependence, and explanations associated with grain boundaries' resistance were made and it seemed that these explanation did work. As a result, there is reason to believe that due to the existence of numerous claw-like barriers in all three orientations, crack growth behaviors show weak orientation dependence for this DS material.

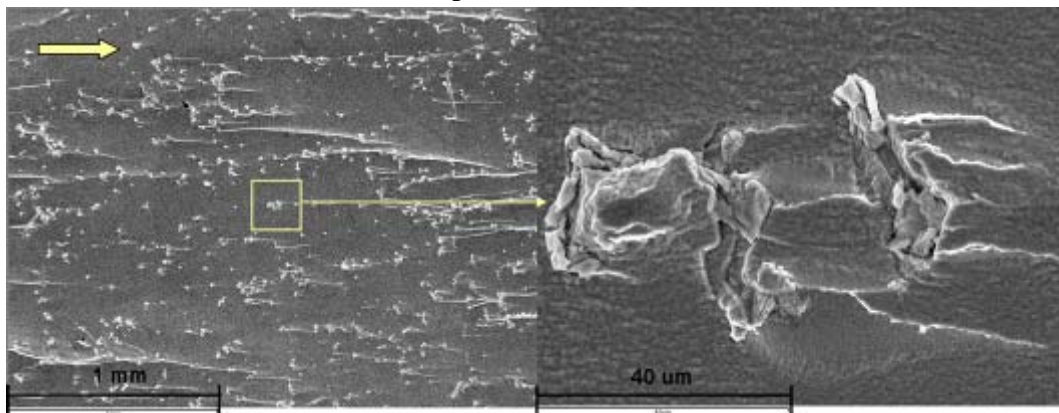


Figure 9. Typical claw-like barriers in the crack path

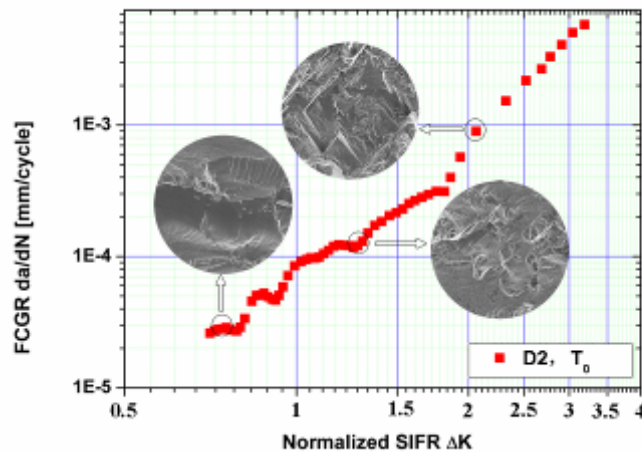


Figure 10. Crack growth rate corresponding to their typical microscopy

To sum up, cracks in all three orientations follow a similar propagation characteristic as ΔK arising. Figure 10 shows the typical microscopy corresponding to different ΔK regimes. It can be seen that as ΔK keeps increasing, the fracture surfaces become rougher and rougher. Meanwhile, more crystal facets appear when ΔK exceeds region II and runs into the fast-propagation region III.

4. Conclusions

Fatigue crack growth behaviors of a newly developed DS superalloy have been studied to investigate the effects of temperatures and orientations. Test specimens were subjected to two temperatures (T_0 and $T_0+250^{\circ}\text{C}$) and three crystal orientations (longitudinal, transverse and diagonal). Following conclusions can be drawn:

- 1) Weak orientation dependence have been found, and all $da/dN - \Delta K$ curves fall into a [1/3,3] narrow bond. Generally cracks in longitudinal and transverse directions have comparable crack growth rate, while those in diagonal direction propagate more slowly, especially in low- ΔK regimes;
- 2) Temperature dependence seems to vary in different orientations, i.e., cracks travel in longitudinal orientation show no temperature dependence, while those in transverse orientations show a little temperature dependence, and temperatures do have large effect on cracks travel in diagonal direction;
- 3) At lower temperatures, stage-I type cracking mode has been found in longitudinal and diagonal directions, while stage-II type cracking mode has been found in transverse direction; Besides, at higher temperatures, stage-II type cracking is preferred in longitudinal and diagonal directions, while stage-I type cracking is preferred in transverse direction.

Acknowledgement

The authors gratefully acknowledge Siemens Energy, Inc. for the support in completing this research; meanwhile, the financial support from National Natural Science Foundation of China (Grant NOs. 10872105 and 51071094) are also appreciated.

Permission for Use:

The content of this paper is copyrighted by Siemens Energy, Inc. and is licensed to CSTAM for publication and distribution only. Any inquiries regarding permission to use the content of this paper, in whole or in part, for any purpose must be addressed to Siemens Energy, Inc. directly.

Reference

- [1] R. B., Scralin. "Fatigue crack propagation in a directionally-solidified nickel-base alloy". Metallurgical Transactions A, 7A(1976) 1535-1541.
- [2] M. Okazaki, T. Tabata, S. Nohmi. "Intrinsic Stage I crack growth of directionally solidified ni-base superalloys during low-cycle fatigue at elevated temperature". Metallurgical Transactions A, 21A(1990) 2201-2208.
- [3] B. Al-Abed, G. A. Webster. "Comparison of creep-fatigue crack growth in a conventionally cast and directionally solidified nickel base superalloy". Proceedings of the fifth international conference on creep and fracture of engineering materials and structures, B. Wilshire and R.W. Evans. Eds, The Institute of Materials, London, 1993(1993) 491-501.
- [4] S. Highsmith. Jr., W. S. Johnson. "Scatter in fatigue crack growth rate in a directionally solidified nickel-base superalloy". Journal of ASTM International, 1(2)(2004) 1-12.
- [5] K. B. Yoon, T. G. Park, A. Saxena. "Elevated temperature fatigue crack growth model for DS-GTD-111". Strength, Fracture and Complexity, 4(2006) 35-40.
- [6] S. Highsmith. Jr., W. S. Johnson. "Elevated temperature fatigue crack growth in directionally solidified GTD-111 superalloy". Fatigue and Fracture of Engineering Materials and Structures, 29(1)(2006) 11-22.
- [7] Annual Book of ASTM Standards, E647, ASTM International.
- [8] K. S. Chan, J. E. Hack, G. R. Leverant. "Fatigue crack propagation in Ni-base superalloy single crystals under multiaxial cyclic loads". Metallurgical Transactions A, 17A(1986) 1739-1750.
- [9] K. S. Chan, J. E. Hack, G. R. Leverant. "Fatigue crack growth in MAR-M200 single crystals". Metallurgical Transactions A, 18a(1987) 581-591.
- [10] K. S. Chan, G. R. Leverant. "Elevated-temperature fatigue crack growth behavior of MAR-M200 single crystals". Metallurgical Transactions A, 18a(1987) 593-602.
- [11] H. Kagawa, Y. Mukai. "The effect of crystal orientation and temperature on fatigue crack growth of ni-based single crystal superalloy". Superalloy 2012: 12th international symposium on superalloys, 2012(2012) 225-233.